Barium-137 nuclear magnetic resonance study in the various phases of $BaTiO_3$

1999 J. Phys.: Condens. Matter 11 871

(http://iopscience.iop.org/0953-8984/11/3/025)

J. Phys.: Condens. Matter **11** (1999) 871–879. Printed in the UK PII: S0953-8984(99)97602-6

Barium-137 nuclear magnetic resonance study in the various phases of $BaTiO_3$

A Taye, G Klotzsche, D Michel, S Mulla-Osman and R Böttcher

University of Leipzig, Faculty of Physics and Geosciences, Linnéstrasse 5, D-04103 Leipzig, Germany

Received 14 September 1998

Abstract. ^{137}Ba quadrupole perturbed NMR measurements on a multidomain crystal were performed in order to determine the quadrupole tensors (which are proportional to the electric field gradient (EFG) tensors) in the tetragonal, orthorhombic and rhombohedral phase of $BaTiO_3$. Because of the relatively large quadrupole splitting, only the central transitions were analysed. By means of the well known Volkoff theory the principal values and the directions of the principal axes were evaluated from the angular dependent NMR spectra. Furthermore, the correct determination of the principal values of the quadrupole tensors has been controlled by means of measurements on polycrystalline $BaTiO_3$ samples of the same origin. The conclusions from the measurements on the multidomain crystals are in very good agreement with the results of ^{137}Ba NMR line shape measurements on powdered samples. Moreover, the NMR studies on the crystal sample allow a study of the domain structure in the different ferroelectric phases in complete agreement with the predictions from symmetry considerations.

1. Introduction

Barium titanate ($BaTiO_3$) is one of the most technologically important and intensively studied substances of all piezoelectric and ferroelectric materials. Although the single-crystal properties of $BaTiO_3$ [1] and the properties of barium-titanate-based ceramics [2, 3] have been investigated in a rather large number of publications, NMR techniques are only used in a few papers in order to study structural or dynamic phenomena.

Probably one reason for this situation is the relatively low NMR absolute sensitivity for ^{137}Ba nuclei (natural abundance of 11.3%) of 7.8×10^{-4} compared with that of the protons. For the ^{135}Ba nuclei the conditions are even worse (6.6% natural abundance, absolute sensitivity of 3.2×10^{-4}) as shown in first systematic ^{135}Ba and ^{137}Ba Fourier transform NMR and NQR studies on barium salts in aqueous solutions and on polycrystalline solids by Lutz and Oehler [4]. NMR measurements on a polycrystalline material of barium titanate in the cubic phase above the Curie temperature ($T_C \approx 408$ K, cubic phase with space group $Pm3m$) have been reported by Forbes *et al* [5]. A first systematic study on single crystals of barium titanate has been performed by Bastow [6]. He measured the EFG tensors of ^{137}Ba and ^{47,49}Ti nuclei in the tetragonal phase (NMR measurements at 296 K) from single-crystal rotation patterns of the central transition. In that paper NMR measurements have also been reported on the temperature dependence of the positions of the central transitions for ^{137}Ba and ^{47,49}Ti nuclei (second-order quadrupole shifts) up to the Curie point, where the shifts vanish abruptly. A more detailed NMR study (^{137}Ba and ^{47,49}Ti) of the cubic-to-tetragonal phase transition was performed by Kanert *et al* [7] on single-domain pure $BaTiO_3$ crystals. They measured the temperature

0953-8984/99/030871+09$19.50

dependence of the observed resonance frequencies between room temperature (tetragonal phase) and ∼700 K and the spin–lattice relaxation times over a wide temperature range (room temperature to 1700 K) in order to study the first-order phase transition at ∼408 K. For the other phases of barium titanate, NMR measurements have not yet been reported. Recently solid-state multinuclear NMR studies of ferroelectric, piezoelectric and related materials were reported by Dec *et al* [8]. High field (14.1 T) ^{47,49}Ti, ^{67}Zn, ^{91}Zr and ^{137}Ba MAS NMR studies at room temperature and pressure were performed for Sr, Ba and Ca titanate, for Sr and Ba zirconate and for various metal oxides. Since the measurements were especially related to the study of isotropic chemical shift values, they are not relevant for the following results.

Therefore, in extension mainly of the former paper by Bastow [6], it is the aim of the present work to measure the EFG tensors at the ^{137}Ba sites in $BaTiO_3$ crystals in the orthorhombic phase (space group $Amm2$, between ∼278 K and 183 K), in the rhombohedral phase (below 183 K, space group $R3m$) and, for comparison, also in the tetragonal phase (space group $P4mm$, between ∼278 and 408 K). For this purpose a multidomain crystal of $BaTiO_3$ is available. Using this crystal it was sufficient to measure only the rotational patterns about the crystallographic c axis of one type of domain in order to obtain all the necessary data to derive the complete EFG tensors from the ^{137}Ba NMR spectra. Since the rotation patterns were only studied for the central transitions, where second-order effects of the quadrupole coupling dominate, additionally the results were controlled by means of ^{137}Ba NMR line shape measurements on a polycrystalline barium titanate sample.

2. Experiment

The $BaTiO_3$ multidomain crystal used in our measurements was grown by Dr J Albers from the University of the Saarland. The crystal was cut in such a way that the tetragonal crystallographic axis c (of one type of domain) is parallel to the sample axis and that the longest edge is along the crystallographic c direction. The ^{137}Ba measurements were run at a resonance frequency of 33.35 MHz on a Bruker MSL 300 NMR spectrometer for the crystal and at a resonance frequency of 55.56 MHz on a Bruker MSL 500 NMR spectrometer for the powder. A quadrupole echo pulse sequence was applied in order to circumvent problems with the dead time. Pulse lengths of 8 μs and of 5.4 μs were used for the $\pi/2$ pulses for the measurements of the single crystal and of the powdered sample, respectively. The temperature was controlled by a Bruker temperature control unit B-VT 2000 with an accuracy of ±2 K in the centre of the r.f. coil (middle of the rectangular crystal).

The angular dependent measurements were run for the tetragonal, the orthorhombic and the rhombohedral phases. Only rotational patterns were measured where the c axis (of the tetragonal phase) is oriented parallel to the rotation axis held perpendicular to the direction of the d.c. magnetic field. The second order shifts of the central transition lines, i.e. the frequencies for the $-1/2 \leftrightarrow +1/2$ transition, were recorded. For further calculations a Cartesian frame x, y, z is used (with $\boldsymbol{a} \parallel x$, $\boldsymbol{b} \parallel y$ and $\boldsymbol{c} \parallel z$) instead of $\boldsymbol{a}$, $\boldsymbol{b}$, $\boldsymbol{c}$. The angular dependent second order quadrupole shifts $\Delta\nu$ were fitted to the known formula (Volkoff theory [9])

$$\Delta\nu = \frac{1}{\nu_L}(n_z + p_z \cos 2\theta_z + r_z \sin 2\theta_z + u_z \cos 4\theta_z + v_z \sin 4\theta_z) \tag{1}$$

where the angle θ_z (rotation angle) between the crystallographic $\boldsymbol{a}$ axis and the external magnetic field was varied in the range from $\theta_z = 0$ to $\theta_z = 210^\circ$ in steps of 3°. The parameters

n_z, p_z etc are defined by the equations

$$\begin{aligned} n_z &= \frac{1}{192}\left\{9V_{zz}^2 - 14\left[\left(\frac{V_{xx}-V_{yy}}{2}\right)^2 + V_{xy}^2\right] - 8(V_{xz}^2 + V_{yz}^2)\right\} \\ p_z &= \frac{1}{32}\{V_{zz}(V_{xx}-V_{yy}) + 4(V_{yz}^2 - V_{xz}^2)\} \\ r_z &= \frac{1}{16}\{-V_{zz}V_{xy} + 4V_{xz}V_{yz}\} \\ u_z &= \frac{3}{32}\left\{\frac{(V_{xx}-V_{yy})^2}{4} - V_{xy}^2\right\} \\ v_z &= -\frac{3}{32}\{(V_{xx}-V_{yy})V_{xy}\} \end{aligned} \tag{2}$$

which are related to the quadrupole tensor elements $V_{ik} = 3eQ\phi_{ik}/[I(2I-1)h]$ (in units of MHz) in the crystallographic axis system. ϕ_{ik} is the electric field gradient (EFG) tensor. In the case of an axially symmetric tensor (especially for the rhombohedral phase) the patterns were also fitted to the analogous expression

$$\Delta\nu = -\nu_Q^2[I(I+1) - \tfrac{3}{4}](1-\mu^2)(9\mu^2-1)/(16\nu_L) \tag{3}$$

where $\nu_Q = 3e^2qQ/[2I(2I-1)h]$, $I = \frac{3}{2}$ for ^{137}Ba nuclei, $\mu = \cos\theta$, θ is the angle between the symmetry axis and the external field, $\phi_{zz} = eq$ is the largest principal value of the EFG tensor, eQ is the quadrupole momentum and ν_L is the Larmor frequency.

The anisotropic components of the chemical shift tensor have been neglected because of their relatively small magnitudes as compared with the quadrupole frequencies ν_Q [6].

3. Results

3.1. Measurements of the quadrupole tensors on multidomain crystals

3.1.1. Tetragonal phase. A typical rotation pattern for the tetragonal phase is shown in figure 1. Clearly a 90° symmetry appears in the spectra, and the fact that one of these curves does not show any angular dependence is in accordance with the existence of three different 90° domains.

Having in mind this domain structure, the fit of the curves to the second order line splitting $\Delta\nu$ is very simple because at first the curve A3 can be used where no angular variation occurs. Here one of the principal axes (X, Y, Z) has to be parallel to the rotation axis. This leads to the principal values

$$V_{XX} = V_{YY} = -1.43 \pm 0.03 \text{ MHz} \qquad V_{ZZ} = e^2qQ/h = 2.86 \pm 0.03 \text{ MHz}$$

with an asymmetry parameter $\eta = (V_{XX} - V_{YY})/V_{ZZ} = 0$ as expected. The values agree with the results in [6]. The usual convention $|V_{XX}| \leqslant |V_{YY}| \leqslant |V_{ZZ}|$ has been applied. The principal axes are parallel to the crystallographic axes $\boldsymbol{a}$, $\boldsymbol{b}$, $\boldsymbol{c}$, i.e. the Euler angles are $\alpha = \beta = \gamma = 0°$ for this case.

The direction of the principal axis with the largest EFG component points from the Ba atom to the next nearest Ba atom, i.e. it is parallel to the [001]-direction and thus parallel to the spontaneous polarization. The other eigenvectors are chosen here to be parallel to the directions [100] and [010] (figure 2(a)). Very simply the other curves (A1, A2) in figure 1 can be explained by the existence of various domains and the respective tensors can be obtained by rotations of 90° around the axes [100] and [010]. In this way the other fit curves for $\Delta\nu$ can be obtained.

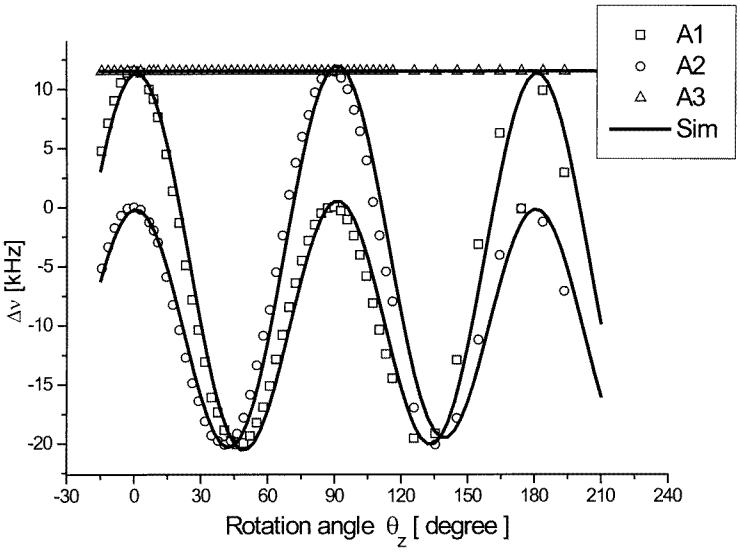

Figure 1. Rotation pattern for the second order quadrupole shift $\Delta\nu$ of the central transitions in the tetragonal phase ($T = 297$ K). The crystal was rotated around the [001] axis and the angle θ_z is the angle between the crystallographic [100] axis and the direction of the external magnetic field with $\theta_z = 0$ for $B_0 \parallel [100]$. The patterns A1, A2 and A3 belong to the different 90° domains. According to the Volkoff theory in second order the fit curves of the angular dependences as shown lead to the same principal values for the quadrupole tensor.

3.1.2. Orthorhombic phase. The angular dependence of $\Delta\nu$ for this phase is shown in figure 3. In the crystal axis system the simulation, for instance of the curve B1, leads to the tensor

$$V_{B1} = \begin{bmatrix} 1.15 & 1.11 & 0 \\ 1.11 & 1.13 & 0 \\ 0 & 0 & -2.28 \end{bmatrix} \tag{4}$$

and the principal values are

$$V_{XX} = -0.03 \pm 0.03 \text{ MHz} \qquad V_{YY} = -2.25 \pm 0.03 \text{ MHz} \qquad V_{ZZ} = 2.28 \pm 0.03 \text{ MHz}$$

with an asymmetry parameter of $\eta = 0.98$. The matrix of the direction cosines is given by

$$E_{B1} = \begin{bmatrix} 0 & 0 & 1 \\ -0.704 & 0.710 & 0 \\ 0.710 & 0.704 & 0 \end{bmatrix}. \tag{5}$$

In agreement with these eigenvectors the Euler angles between the crystal axis system and the principal axis system (X, Y, Z) are $\alpha = 45°$, $\beta = 90°$ and $\gamma = 180°$. The largest principal axis is in the direction from a Ba to an oxygen atom in the middle of an edge of the unit cell, i.e. it is parallel to [110], the axis with V_{YY} is parallel to $[\bar{1}10]$ and the axis with V_{XX} points to a neighbouring Ba atom parallel to [001]. The bond direction from a Ba to an O atom is the direction of the face diagonal (figure 2(b)).

All the other rotation patterns in figure 3 can be explained by the same principal values if again the existence of the various domains is taken into account. Hence, if the tensor (4) is subsequently rotated by 90° about the axes [001], [100] and [010], then the curves B2, B3 and B4, respectively, can completely be described. The complete simulations are shown in figure 3 where the rotation patterns for the latter two are difficult to separate, but their ascription is

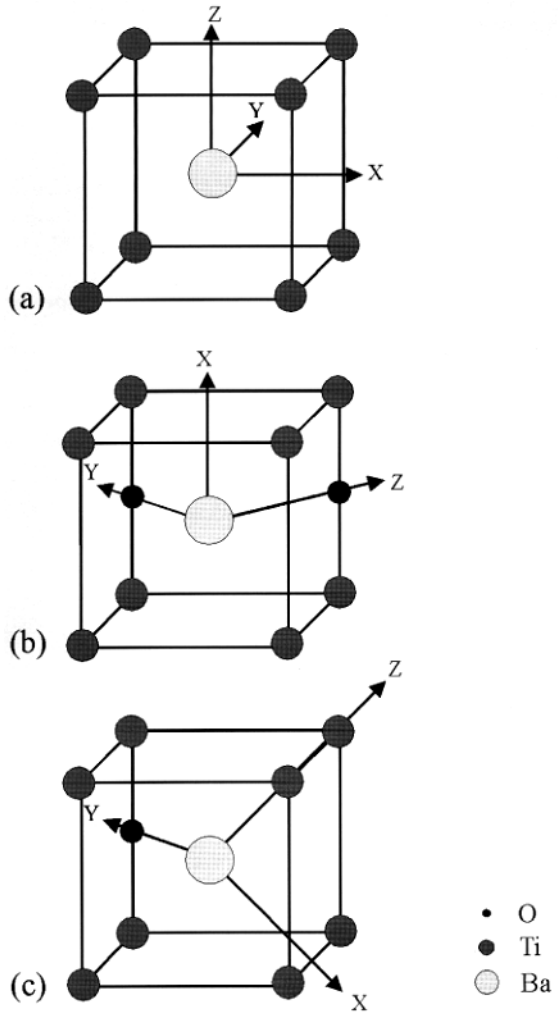

Figure 2. Orientation of the quadrupole tensor in the unit cell: (a) tetragonal, (b) orthorhombic and (c) rhombohedral phase. A unit cell is chosen where the Ba atom is surrounded by eight Ti atoms.

supported by symmetry arguments. Because of the rotation axis chosen in the experiments only four out of the six domain directions can be differentiated. The four domain directions are [110], [1$\bar{1}$0], [101] and [011]. The domain structure is in complete agreement with the known 60°, 90°, 120° and 180° domains for $BaTiO_3$ in this phase [10, 11].

3.1.3. Rhombohedral phase. The rotation patterns are shown in figure 4. For the evaluation of the EFG tensors we started with an axial tensor ($\eta = 0$) according to the symmetry. For the line C2 we found the tensor elements

$$V_{C2} = \begin{bmatrix} -0.001 & 1.029 & 1.031 \\ 1.029 & -0.001 & 1.031 \\ 1.031 & 1.031 & 0.002 \end{bmatrix} \tag{6}$$

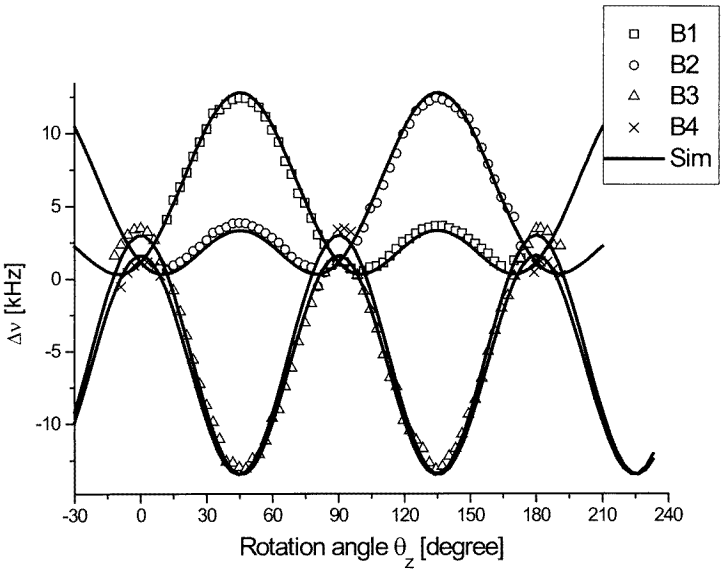

Figure 3. Rotation pattern for the second order quadrupole shift $\Delta\nu$ of the central lines in the orthorhombic phase. The crystal is rotated around the [001] direction. The angle θ_z is defined as explained in the text. The principal values of the tensors are the same in all the fits, and the curves B1, B2, B3 and B4 reflect four different domains. The temperature of the measurements is 260 K.

in the crystallographic frame. The problem with this simulation was that only a rather bad accuracy could be achieved. This is due to the fact that the diagonal tensor elements in the crystallographic frame were very small with respect to the off-diagonal ones. Hence only a rough estimation of them was possible because they could not be put to zero. To improve the accuracy, equation (3) was applied where the angle was chosen in an appropriate way. The principal tensor elements found this way are $V_{XX} = V_{YY} = -1.03 \pm 0.03$ MHz and $V_{ZZ} = 2.06 \pm 0.03$ MHz. The matrix of the direction cosines of the quadrupole tensor for the Ba nuclei belonging to the curve C2 is given by

$$E_{C2} = \begin{bmatrix} -0.409 & -0.409 & 0.816 \\ -0.707 & 0.707 & 0 \\ 0.577 & 0.577 & 0.577 \end{bmatrix} \tag{7}$$

which leads to the Euler angles of $\alpha = 45^\circ$, $\beta = 54.7^\circ$ and $\gamma = 0^\circ$. The axis with the largest principal value is along the bond direction between the Ba and the Ti atoms (parallel to [111]). The direction for V_{YY} is parallel to [110], i.e. it lies in the plane (111) and points towards an O atom (figure 2(c)).

For the interpretation of all the rotation patterns again the existence of different domains was considered. Taking equal principal values of the EFG tensors for all patterns and suitably chosen angles for the rotation of the tensor axes, a good agreement with the experimental results could be achieved. Thus, the existence of 70.5°, 109.5° and 180° domains [11] is completely consistent with our ^{137}Ba NMR measurements in the rhombohedral phase.

3.2. Measurements on polycrystalline samples

In order to confirm the results obtained for the principal values of the tensors from the single crystal measurements, the ^{137}Ba NMR line shape for the powder samples was studied. For

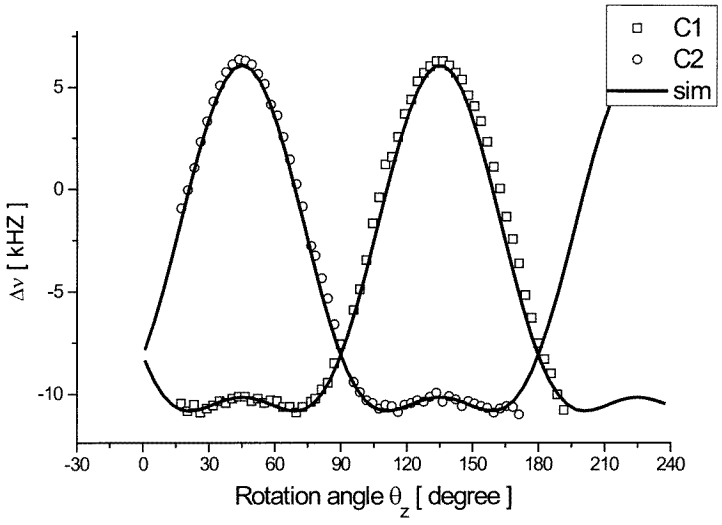

Figure 4. Rotation pattern and simulations for the second order quadrupole shift $\Delta\nu$ of the central lines for the rhombohedral phase. The principal values of the tensor are equal for all curves which differ only in the directions of the domains. The crystal was rotated about the [001] direction (of the cubic phase). θ_z is the angle between the direction of the magnetic field B_0 and [100]. The measurement was performed at 160 K.

Table 1. Quadrupole coupling constants (in MHz) and asymmetry parameters as derived both from crystal and powder measurements of $BaTiO_3$ in the different phases.

	Tetragonal	Orthorhombic	Rhombohedral
Crystal	$V_{ZZ} = 2.86$	$V_{ZZ} = 2.28$	$V_{ZZ} = 2.06$
	$\eta = 0$	$\eta = 0.98$	$\eta = 0$
Powder	$V_{ZZ} = 2.86$	$V_{ZZ} = 2.20$	$V_{ZZ} = 2.09$
	$\eta = 0$	$\eta = 0.98$	$\eta = 0$

the tetragonal, orthorhombic and rhombohedral phases the spectra are shown in figure 5 respectively. The parameters derived by a simulation of the experimental line shapes prove the results from the measurements on the multidomain crystal (table 1). The simulations were carried out by means of the program 'WINFIT' (Bruker). A more detailed inspection of the line shape simulations reveals that in particular the edges of the powder line shapes are in a very good agreement with the results of the simulations. The distribution functions between the singularities of the line shapes show deviations which can simply be explained by an incomplete averaging over the different angles. This is due to the fact that we used relatively large crystallites (with diameters of about 500 μm) which we produced from our $BaTiO_3$ crystals by means of a mortar. Because of the relatively small total amount of polycrystalline material for the measurements an incomplete averaging cannot be excluded. Otherwise, the use of larger diameters of the particles has led to relatively sharp singularities in the powder spectra, which enable an unambiguous interpretation of the line shapes. Furthermore it excludes that size effects of the $BaTiO_3$ particles play a role in the spectra, which will be described in a forthcoming paper.

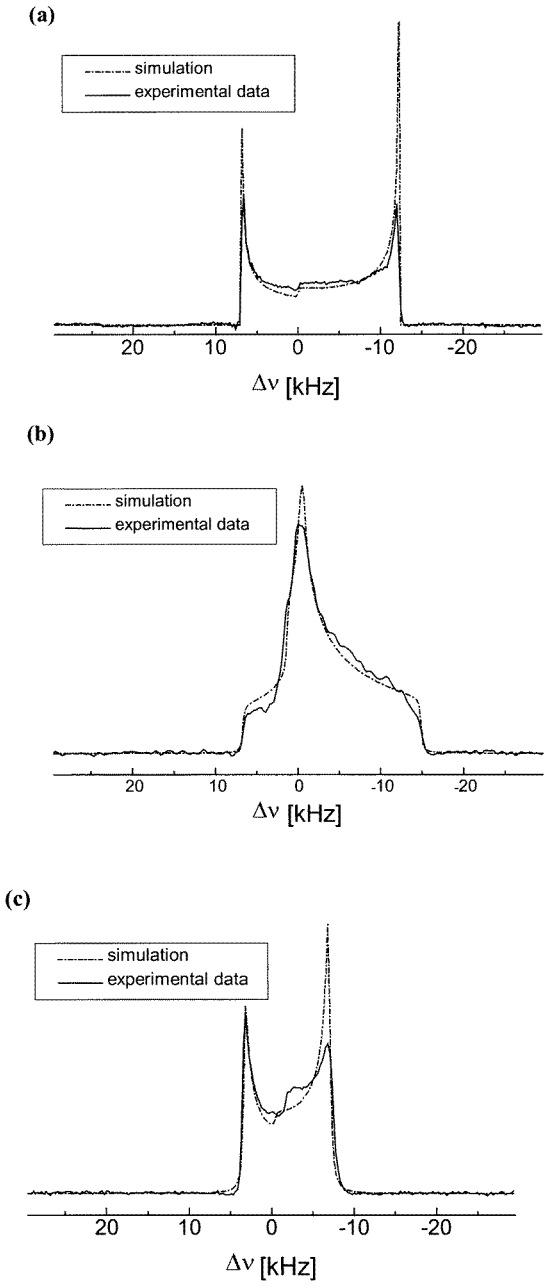

Figure 5. ^{137}Ba-NMR spectrum of a polycrystalline sample of $BaTiO_3$: (a) tetragonal phase at 297 K, (b) orthorhombic phase at 260 K and (c) rhombohedral phase at 160 K. The measurements were run at a Larmor frequency of 55.56 MHz.

4. Conclusions

The experimental results obtained in this work reflect clearly the changes of symmetry in the rhombohedral, orthorhombic and tetragonal phases. Because of the large quadrupolar constant

it was not possible to measure satellite lines which are determined by first order perturbation theory.

Quadrupole perturbed NMR measurements on the multidomain crystal show a significant change of the direction of the EFG tensor in the various phases. Furthermore they allow us to deduce the domain structure in the various ferroelectric phases from the rotational patterns.

The previously reported results [10, 11] about the domains for the tetragonal, the orthorhombic and the rhombohedral phase are in complete agreement with our ^{137}Ba NMR measurements on a multidomain crystal.

In all cases we found an agreement between the direction of the largest principal axis of the quadrupole tensor and the spontaneous polarization [11].

The results point out a significant difference of the asymmetry parameter η (in agreement with symmetry requirements) and a change of the quadrupolar constant e^2qQ/h in the various ferroelectric phases.

The investigations on powdered samples support the results obtained for the single crystal.

The conclusions from the NMR measurements are in agreement with previously reported results of optical, dielectric and XRD studies [10, 12–15].

Acknowledgments

We are greatly indebted to Dr J Albers from the University of the Saarland who provided us with the $BaTiO_3$ crystal.

References

[1] Burns G and Glazer A M 1990 *Space Groups for Solid State Scientists* (San Diego: Academic)
[2] Kanata T, Yoshikawa T and Kubota K 1987 *Solid State Commun.* **62** 765–67
[3] McHale J M, McIntyre P C, Sickafus K E and Coppa N V 1996 *J. Mater. Res.* **11** 1199
[4] Lutz O and Oehler H 1978 *Z. Phys.* A **288** 11–15
[5] Forbes C E, Hammond W B, Cipollini N E and Lynch J F 1987 *J. Chem. Soc. Chem. Commun.* 433–6
[6] Bastow T J 1989 *J. Phys.: Condens. Matter* **1** 4985
[7] Kanert O, Schulz H and Albers J 1994 *Solid State Commun.* **91** 6465–9
[8] Dec S F, Davis M F, Maciel G E, Bronnimann C E, Fitzgerald J J and Han S S 1993 *Inorg. Chem.* **32** 955–9
[9] Volkoff G M 1953 *Can. J. Phys.* **31** 820
[10] Rhodes R G 1951 *Acta Crystallogr.* **4** 105
[11] Kuhn W J 1991 *Ferroelectr. Lett.* **13** 101–8
[12] Forsbergh P W Jr 1949 *Phys. Rev.* **76** 1187
[13] Jona F and Pepinsky R 1957 *Phys. Rev.* **105** 861
[14] Mathias B and von Hippel A 1948 *Phys. Rev.* **73** 1378
[15] Walter J M 1949 *Phys. Rev.* **76** 1221